High Performance and Increased Precision Techniques for Feynman Loop Integrals

K Kato[1], E de Doncker[2], T Ishikawa[3], J Kapenga[2], O Olagbemi[2] and F Yuasa[3]

[1] Department of Physics, Kogakuin University, Shinjuku, Tokyo 163-8677, Japan

[2] Department of Computer Science, Western Michigan University, 1903 W. Michigan Avenue, Kalamazoo, MI 49008, United States

[3] High Energy Accelerator Research Organization (KEK), 1-1 Oho Tsukuba, Ibaraki 305-0801, Japan

E-mail: `kato@cc.kogakuin.ac.jp`

Abstract. For the investigation of physics within and beyond the Standard Model, a precise evaluation of higher order corrections in perturbative quantum field theory is required. We have worked on the development of a computational method for Feynman loop integrals with a fully numerical approach. It is based on numerical integration and extrapolation techniques. In this paper, we describe the status and new developments in our techniques for the numerical computation of Feynman loop integrals.

Separation of ultra-violet divergences is important for the renormalization procedure. In our analyses, the separation can be done numerically. For 2-loop integrals we have performed the calculations for up to 4-point functions, and for 2-point functions we can handle up to 4-loop integrals. We report the status and accuracy of the computations with detailed numerical comparisons to results in the literature, in order to demonstrate that our method will evolve into an important component of automated systems for the study of higher-order radiative corrections.

1. Introduction

In high energy physics, we encounter the need for large-scale computations to obtain the theoretical prediction required to study experimental data. When the number of final particles is large, the matrix element and phase space becomes complicated and lengthy. When good experimental data are available, i.e., data are of high statistical quality, the higher-order radiative correction is mandatory. Such a large-scale computation is generally beyond man-power calculation, so that automated systems to calculate the perturbative expansion in quantum field theory (QFT) prove to be an essential tool for the present and future high-energy experiments.

Perturbation calculations in QFT follow a well established algorithm and many systems are already provided for practical use to analyze experimental data. For the radiative corrections, the one-loop order calculation is incorporated in several systems, GRACE [1], CompHEP [2], FeynArt/Calc [3], FDC [4], and so forth. Considering future accelerator experiments, the development of a system to perform computations beyond one-loop will be of great importance. One indispensable component of such a system is a library of multi-loop integrals. The library should be robust and general to treat any combination of internal masses and external momenta.

While the analytical calculation of multi-loop integrals is studied by many authors [5], the analytic expression for the most general form seems to be far from accomplished. Therefore we have started to solve the problem by numerical methods.

2. Computational method for loop integrals
The integral we study is

$$I = (-1)^N \frac{\Gamma(N - nL/2)}{(4\pi)^{nL/2}} \int \prod dx_r \frac{\delta(1 - \sum x_r)}{U^{n/2}(V - i\rho)^{N-nL/2}} \tag{1}$$

where n is the space-time dimension, N is the number of propagators, L is the number of loops and

$$V = M^2 - \frac{W}{U}, \qquad M^2 = \sum_r x_r m_r^2. \tag{2}$$

Here the functions U and W are polynomials in the integration variables x_r, and are derived from the structure of the graph. The coefficients of the W polynomial are determined by the external momenta and internal masses.

In the analytic method, one needs a sophisticated variable transformation of the x_r. However, we dare not exploit the transformation since the library is intended as a component of an automated system where the integrand will be supplied by the automatic diagram generator, so that the assignment of the x_r and other elements may not be under our control.

When a Feynman diagram includes fermions and/or gauge bosons, the integral has a momentum dependent numerator. Although the integral studied here is of scalar type, the introduction of a numerator does not cause a serious problem (although it may make the numerical integration more computationally intensive).

We introduce dimensional regularization to handle ultraviolet divergence, i.e., by setting

$$n = 4 - 2\varepsilon. \tag{3}$$

In the numerical evaluation of Eq.(1), we might encounter a singularity for $\rho \to 0$ and/or for $\varepsilon \to 0$. In the analytical treatment of loop integrals, the singularity for $\rho \to 0$ can be avoided by analytic continuation. However, in the numerical method, if we calculate Eq.(1) by naively taking $\rho = 0$, the result may be divergent or unstable. We have developed the direct computation method (DCM) to manage the problem [6, 7, 8, 9]. In DCM, we keep the numerical value of ρ non-zero. This value is not necessarily very small. When ρ is finite, Eq.(1) can be computed numerically as a function of ρ. For a sequence of $\rho = \rho_k$, $k = 1 \ldots K$, we obtain a sequence of numerical values $I(\rho_k)$, $k = 1 \ldots K$. From this sequence we can estimate the integral I either by a nonlinear extrapolation with Wynn's algorithm (ϵ algorithm) [12], or by using a linear solver. Note that a geometric sequence is needed when using the ϵ algorithm.

In this paper, we discuss the singularity as $\varepsilon \to 0$, originating from the ultra-violet (UV) singularity. The infrared singularity also appears as a pole in ε. As the latter is already studied in [8], we concentrate here on the UV-pole. The UV pole in Eq.(1) originates from the Gamma function and/or the integral.

Generally the integral I can be expanded as

$$I = \cdots + \frac{C_{-2}}{\varepsilon^2} + \frac{C_{-1}}{\varepsilon} + C_0 + C_1\varepsilon + C_2\varepsilon^2 + \cdots \tag{4}$$

and we extract the coefficients C_j numerically using the same methods as for the case of $\rho \to 0$, i.e., by linear or nonlinear extrapolation.

3. Numerical results

Using our numerical method, we have computed 2-loop diagrams with up to 4 external lines, and self-energy diagrams with up to 4 loops. The results are compared with those in the literature and show good agreement. As described in the sections below, we use various integration libraries, acceleration and hardware platforms, and check the efficiency and convergence behavior of the computation.

3.1. 4-loop self-energy integrals

We study the diagrams in Fig.1. The integral part is finite, and the Gamma factor is divergent for Fig.1(1) and (2). We consider massless internal particles and $p^2 = 1$ for comparison with the results in [15].

Results are shown in Table 1. The parallel execution time for Table 1(1) is 48s with ParInt [10], using 64 MPI [11] processes on four 16-core nodes of the *thor* cluster at Western Michigan University. The integration for Table 1(2) is performed in 4.8h elapsed time for a 64-thread computation using a double-exponential integration formula (DE) [13] on SR-16000. Fig.1(3) and (4) are also calculated with ParInt on the *thor* cluster.
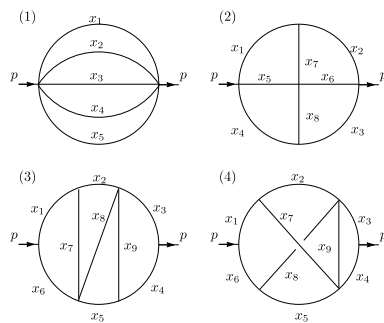

Figure 1. 4-loop self-energy diagrams

Table 1. 4-loop self-energy integrals for Fig.1. The rows with BC list results of [15].

	C_{-1}	C_0	C_1
Fig.1(1)	-0.001736111111109	-0.016927083381	-0.011842916
Fig.1(1) BC	-0.001736111111111	-0.016927083333	-0.011842930
Fig.1(2)	5.1846392	-2.582434	70.39877
Fig.1(2) BC	5.18463877	-2.5824360	70.399151
Fig.1(3)	–	55.585150	Not yet
Fig.1(3) BC	–	55.5852539	
Fig.1(4)	–	52.017714	Not yet
Fig.1(4) BC	–	52.017868	

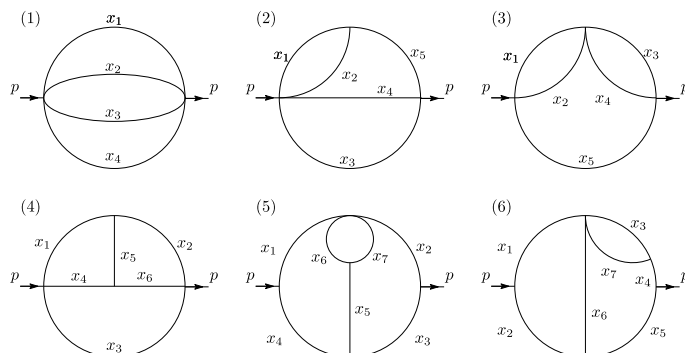### 3.2. 3-loop self-energy integrals

Figure 2. 3-loop self-energy diagrams

Table 2. 3-loop self-energy integral for Fig.2(5). The row marked L gives the results of [14].

	C_{-1}	C_0
Fig.2(5)	0.92370	-2.4201
Fig.2(5) L	0.923631827	-2.42349163

We deal with the diagrams in Fig.2 where maximally a $\frac{1}{\varepsilon^3}$ singularity appears, corresponding to a double-pole divergence ($\sim \frac{1}{\varepsilon^2}$).

As an example, we show the results for Fig.2(5), *ladybug*. To compare with [14], we let $m_r = 1$, $p^2 = 1$. The Gamma factor is finite and the integral is single-pole divergent ($\sim \frac{1}{\epsilon}$). This calculation is carried out with DE and performed in quadruple precision on (dual) E5-2687W v3 @ 3.10GHz using 40 threads. Extrapolated results obtained with Wynn's algorithm are shown for Fig.2(5) in Table 2. Computations for the other diagrams in Fig.2 result in a similar agreement with [14].

3.3. 2-loop vertex integrals

As an example, we consider the diagram in Fig.3(1), which has UV divergence from both the Gamma function and a single pole in the integral part. In total, it is divergent as $\frac{1}{\varepsilon^2}$.

For the numerical computation, we take $m_r = 1$, $p_1^2 = p_2^2 = p_3^2 = 1$, so that there is no singular threshold. In Table 3 we show the convergence behavior of the C coefficients, where a linear solver is used to estimate the coefficients. The bottom row of the table lists the values from [14].

The diagram of Fig.3(2) is also studied and the result for C_{-1} is in good agreement with [14].
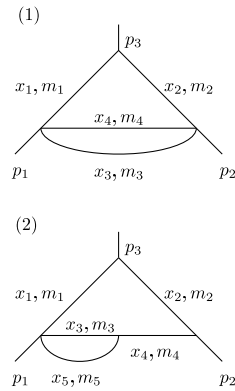
Figure 3. 2-loop vertex diagrams

Table 3. 2-loop vertex integral for Fig.3(1). An integration is performed for each $\varepsilon_j = 1/b_j$ in the first column, and the four coefficients are estimated by a linear extrapolation.

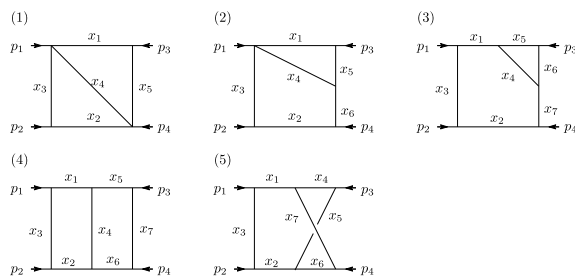| b_j	T [s]	C_{-2}	C_{-1}	C_0	C_1
3	1.4				
4	1.5	0.514890217	0.535680679		
6	1.8	0.505861627	0.598880809	-0.108343080	
8	5.2	0.501111606	0.660631086	-0.364844229	0.342001531
12	2.5	0.500159017	0.680635463	-0.515353351	0.822106580
16	4.2	0.500017647	0.685300679	-0.573315125	1.161395016
24	20.5	0.500001357	0.686098882	-0.588595022	1.307352233
32	19.1	0.500000078	0.686192225	-0.591298134	1.347594589
48	8.6	0.500000001	0.686200327	-0.591641476	1.355242242
[14]		0.5	0.686200636	-0.591666701	1.356196533

3.4. 2-loop box integrals

Figure 4. 2-loop box diagrams

Table 4. 2-loop box integrals for Fig.4. Listed are: integral dimension, error tolerance, maximum number of integral evaluations, sequential and parallel time (in seconds), and parallel speedup, $R = T_1/T_{64}$.

	D.	Tol.	Eval.	T_1 [s]	T_{64} [s]	R
Fig.4(1)	5	10^{-10}	400M	32.6	0.74	44.1
Fig.4(2)	6	10^{-9}	3B	213.6	5.06	42.2
Fig.4(3)	7	10^{-8}	5B	507.9	8.83	57.5
Fig.4(4)	7	10^{-8}	2B	189.9	4.33	43.9
Fig.4(5)	7	10^{-7}	300M	27.6	0.49	56.3
Fig.4(5)	7	10^{-9}	20B	1893	34.6	54.7

Finally, we show results for the box diagrams in Fig.4. These are not UV divergent; the computation is done with $\varepsilon = 0$. Furthermore, the test integral is calculated in the unphysical region, $m_r = 1$, $s = t = 1$, $p_j^2 = 1$, so that it is possible to take $\rho = 0$. The comparison with [14] was shown before in [7].

Here, we report the speedup of the parallel computation on MPI [11]. We use ParInt on the *thor* cluster at Western Michigan University. As shown in Table 4, we gain significant acceleration with 64 processes. The computation times with one process (T_1) and with 64 processes (T_{64}) are given in seconds (s), and the speedup is $R = T_1/T_{64}$.

4. Summary

Numerical methods are tested to calculate loop integrals with 2 to 4 loops, and up to 4-point functions. In parameter space, up to 8-dimensional integrals are computed. The DCM method works to estimate both UV-divergent and finite terms using dimensional regularization. As the approach is expected to be part of an automated system, no special handling of the integrand is utilized. Automatic decisions on the variable transformation might improve the status. Problems with large CPU-times can be targeted using suitable parallel software and platforms. The study should be extended to the general cases with physical masses and external momenta, including a numerator part in the integrand function.

Acknowledgments

References

[1] Khiem P H, Fujimoto J, Ishikawa T, Kaneko T, Kato K, Kurihara Y, Shimizu Y, Ueda T, Vermaseren J A M and Yasui Y 2013 Eur. Phys. J. C 73:2400
[2] Boos E, Bunichev V, Dubinin M, Dudko L, Edneral V, Ilyin V, Kryukov A, Savrin V, Semenov A and Sherstnev A 2008 PoS ACAT08:008
[3] Hahn T 2010 PoS ACAT2010:078
[4] Wang J-X 2004 Nucl. Instrum. Meth. A534 241-245
[5] See, for an instance, other papers in the proceedings of ACAT2016 in track 3.
[6] de Doncker E, Yuasa F and Assaf R 2013 Journal of Physics: Conf. Ser. 454 doi:10.1088/1742-6596/454/1/012082
[7] de Doncker E and Yuasa F 2014 XV Adv. Comp. and Anal. Tech. in Phys. Res., Journal of Physics: Conference Series (ACAT 2013) 523 doi:10.1088/1742-6596/523/1/012052
[8] de Doncker E, Fujimoto J, Hamaguchi N, Ishikawa T, Kurihara Y, Shimizu Y and Yuasa F 2011 Journal of Computational Science (JoCS) 3 102-112 doi:10.1016/j.jocs.2011.06.003
[9] Yuasa F, de Doncker E, Hamaguchi N, Ishikawa T, Kato K, Kurihara Y, Fujimoto J and Shimizu Y 2012 Computer Physics Communications 183 2136-2144
[10] ParInt http://www.cs.wmich.edu/parint
[11] Open-MPI http://www.open-mpi.org
[12] Wynn P 1956 Mathematical Tables and Aids to Computing 10 91-96
[13] Takahasi H and Mori M 1974 Publications of the Research Institute for Mathematical Sciences 9 721-741
[14] Laporta S 2000 Int. J. Mod. Phys. A 15 5087-5159 arXiv:hep-ph/0102033v1
[15] Baikov B A and Chetyrkin K G 2010 Nuclear Physics B 837 186-220